◆ Human Brain Mapping 36:2719–2731 (2015) ◆

Interactions Between Default Mode and Control Networks as a Function of Increasing Cognitive Reasoning Complexity

Luke Hearne,[1] Luca Cocchi,[1]* Andrew Zalesky,[2] and Jason B. Mattingley[1,3]

[1]*Queensland Brain Institute, The University of Queensland, Brisbane, Australia*
[2]*Melbourne Neuropsychiatry Centre and Melbourne School of Engineering, The University of Melbourne, Melbourne, Australia*
[3]*School of Psychology, The University of Queensland, Brisbane, Australia*

Abstract: Successful performance of challenging cognitive tasks depends on a consistent functional segregation of activity within the default-mode network, on the one hand, and control networks encompassing frontoparietal and cingulo-opercular areas on the other. Recent work, however, has suggested that in some cognitive control contexts nodes within the default-mode and control networks may actually cooperate to achieve optimal task performance. Here, we used functional magnetic resonance imaging to examine whether the ability to relate variables while solving a cognitive reasoning problem involves transient increases in connectivity between default-mode and control regions. Participants performed a modified version of the classic Wason selection task, in which the number of variables to be related is systematically varied across trials. As expected, areas within the default-mode network showed a parametric deactivation with increases in relational complexity, compared with neural activity in null trials. Critically, some of these areas also showed enhanced connectivity with task-positive control regions. Specifically, task-based connectivity between the striatum and the angular gyri, and between the thalamus and right temporal pole, increased as a function of relational complexity. These findings challenge the notion that functional segregation between regions within default-mode and control networks invariably support cognitive task performance, and reveal previously unknown roles for the striatum and thalamus in managing network dynamics during cognitive reasoning. *Hum Brain Mapp 36:2719–2731, 2015.*

Key words: relational complexity; reasoning; connectivity; networks; default-mode; cognitive control

Additional Supporting Information may be found in the online version of this article.

Contract grant sponsor: Australian Research Council (ARC) Science of Learning Research Centre; Contract grant number: SR120300015 (to J.B.M.); Contract grant sponsor: ARC Centre of Excellence for Integrative Brain Function; Contract grant number: CE140100007; Contract grant sponsor: ARC Australian Laureate Fellowship; Contract grant number: FL110100103; Contract grant sponsor: Australian National Health Medical Research Council; Contract grant number: APP1047648 (to A.Z.)
Conflict of interest: None

Luke Hearne and Luca Cocchi contributed equally to this work.

*Correspondence to: Luca Cocchi, Queensland Brain Institute, The University of Queensland. St Lucia, QLD 4072, Australia. E-mail: l.cocchi@uq.edu.au or lcocchi78@gmail.com

Received for publication 21 January 2015; Revised 9 March 2015; Accepted 15 March 2015.

DOI: 10.1002/hbm.22802
Published online 2 April 2015 in Wiley Online Library (wileyonlinelibrary.com).

INTRODUCTION

The execution of increasingly demanding cognitive tasks, such as logical problem solving, has been associated with proportional increases in neural activity and functional connectivity in frontoparietal and cingulo-opercular control networks [Cocchi et al., 2014; Dosenbach et al., 2010]. Increased task difficulty is also associated with decreases in neural activity within regions encompassing the default-mode network [Lawrence et al., 2003; McKiernan et al., 2003]. An increase in functional antagonism (i.e., anticorrelation) between activity in control and default-mode regions as a function of increased task demands is thought to be critical for optimal cognitive performance [Anticevic et al., 2012; Fox et al., 2005; Kelly et al., 2008; Sonuga-Barke and Castellanos, 2007; Weissman et al., 2006].

Recent evidence from functional neuroimaging studies suggests that cognitive processes such as reasoning, attention and memory recall are supported by complex reconfigurations in the patterns of cooperation and competition between widespread resting-state networks [Cocchi et al., 2013; Dwyer et al., 2014; Leech et al., 2011, 2012]. Such changes in neural network dynamics preserve the general functional network architecture of the brain [Cole et al., 2014], appear task-specific [Cocchi et al., 2014; Cole et al., 2013; Sridharan et al., 2008], and may include cooperation between regions and networks that are otherwise functionally segregated in the resting state [Bluhm et al., 2011; Dwyer et al., 2014; Fornito et al., 2012; Leech et al., 2011; Liang et al., in press; Popa et al., 2009]. This research suggests that cognitive task performance does not necessarily require antagonism between default-mode and control networks [Anticevic et al., 2012; Sonuga-Barke and Castellanos, 2007].

We recently demonstrated that the process of actively relating variables to solve logical reasoning problems involves enhancement of neural activity and task-based connectivity between discrete regions within the frontoparietal and cingulo-opercular control networks [Cocchi et al., 2014]. The ability to relate multiple variables to achieve internal goals is a critical component of human intelligence [Johnson-Laird, 2010], and has been formally quantified with the relational complexity metric [Halford et al., 1998, 2010]. The task used in our study was an adaptation of the Wason selection task (WST), a classic deductive reasoning paradigm [Wason, 1966] (Fig. 1a). In this paradigm, participants are asked to test if a given set of propositions could potentially disconfirm a logical rule (Fig. 1b). Our original analysis focused exclusively on positive, complexity-evoked changes in local activity and connectivity, compared with task unrelated activity. Here, we undertook new analyses of these data to directly assess complexity-induced changes in dynamics between control and default-mode regions. Our aim was to determine whether complexity in relational reasoning is supported by a consistent increase in competition (i.e., anticorrelation), or selective integration, between regions encompassing control and default-mode networks. By testing these competing predictions, our study provides critical information for understanding task-evoked neural dynamics supporting complex reasoning processes.

MATERIALS AND METHODS

Participants

Twenty-one participants aged from 21 to 39 years (mean $\pm$ SD = 28.6 $\pm$ 5.0 years, 12 females) were included in the analysis [Cocchi et al., 2014]. Participants provided informed written consent to participate in the study. The study was approved by The University of Queensland Human Research Ethics Committee and conducted in accordance with the Declaration of Helsinki.

Paradigm

In the classic WST participants are shown four cards and provided with a conditional rule (Fig. 1a). Participants are then asked which card(s) must be turned over to disconfirm the rule. To solve the WST, the participant must consider each card's relationship with the rule, and determine whether the card can disconfirm it [Wason, 1968].

In the current study, we implemented an adapted version of the WST (Fig. 1b). The key difference between the original version of the task and the one used in our study is that the rules and "cards" were presented sequentially, and that only one card was assessed on each trial (rather than all four simultaneously). The task involved presentation of a logical rule (3,000 ms) that established a defined relationship between two alphanumeric variables (e.g., "If A then 7"). Rules always consisted of a single letter and a single digit (from 1 to 9). Letters and digits were presented with equivalent frequency as the first and second elements of the rule. One hundred and eighty different rules were presented throughout the experiment. As such, it was not possible for participants to reduce the task to a mere matching of elements. Following a variable 3,000–5,000 ms period, a single letter (on 50% of the trials) or number was displayed for 3,000 ms. Participants were asked to think of this character as one side of a card and to indicate, as quickly and accurately as possible, if the card could disconfirm the rule, assuming the other side of the card could contain any possible number (if the face side contained a letter) or letter (if the face side contained a number). Importantly, participants were instructed that the rule was not bidirectional. For example, the rule "If A then 7" does not imply "If 7 then A."

Five unique card conditions were presented (see Table I for an example of each). In accordance with the relational complexity metric [Halford et al., 2010], each condition had a specific level of complexity: (i) Binary. The card presents an element that corresponds to the first element of the rule. (ii) Inverse binary. The card presents an

element that corresponds to the second element of the rule. (iii) Ternary. The card element is different from the first element of the rule, but of the same category (i.e., a letter or number). (iv) Quaternary. The card presents an element that is different to the second element of the rule, but of the same category. (v) Active control. The active control condition involved the presentation of a nonalphanumeric element completely unrelated to the rule (e.g., #). Lastly, the paradigm included null trials in which a white fixation cross was presented for the whole duration of the trial. Participants were instructed to rest and do nothing when presented with a null trial. These six trial types were presented with equal frequency in pseudorandom order across five runs lasting approximately 10 min, each consisting of 36 task trials. Before performing the task in the MR scanner participants performed a training session. In this practice session, the relations to be established to solve the different card conditions were explained [further details in Cocchi et al., 2014].

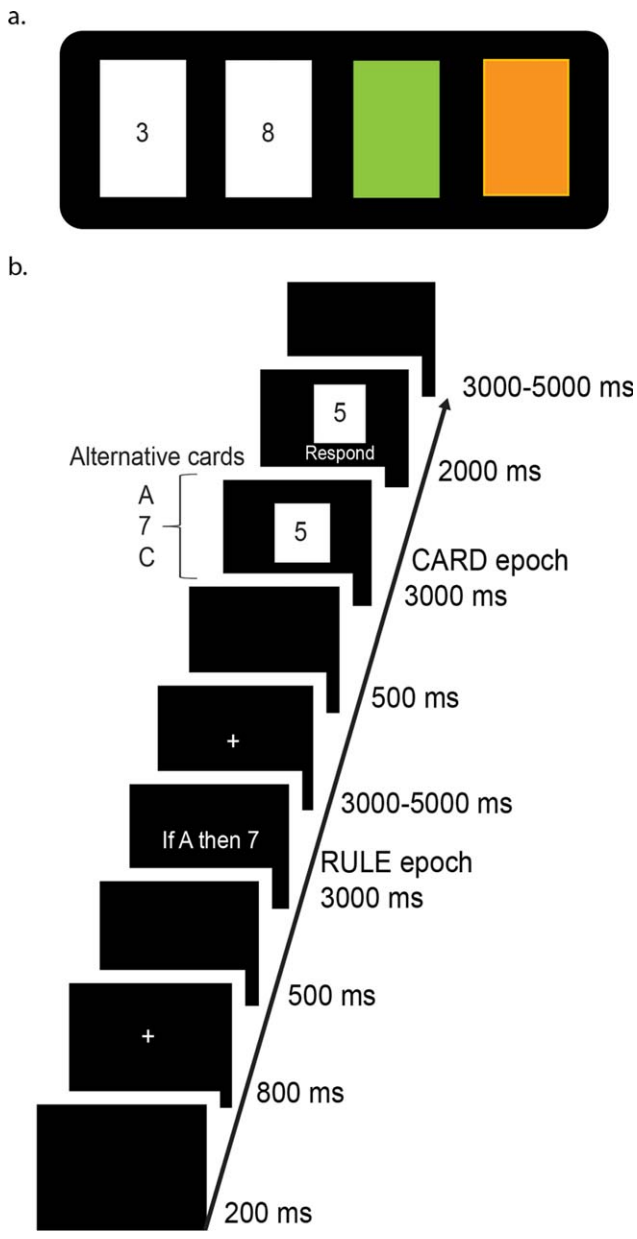

Imaging

The study was conducted using a 3T Siemens Trio scanner (32 channel head coil, TR = 2,550 ms; TE = 32 ms; flip angle = 90°, FOV = 210 × 210 mm, 36 axial slices). Images were preprocessed using a standard pipeline implemented in the software SPM8 [for details see Cocchi et al., 2014]. This pipeline comprised a correction for acquisition time, realignment, normalization, high-pass filtering, and a correction for first-order autocorrelations. Analyses comprised the assessment of neural activity and task-based functional connectivity related to the processing of increasingly complex card stimuli. Regional activity was isolated using a general linear model framework (GLM), as implemented in SPM8. At the first level, conditions of interest were modeled as boxcar functions convolved with a canonical hemodynamic response function and its temporal derivative. The model included the rule epochs and the card-processing epoch (3,000 ms) for all six conditions (the four card types, plus the control, and null trials). Errors due to increased relational complexity were one of our predictors for changes in brain activity and connectivity; as such, the card regressors included both correct and incorrect trials. We also performed the analysis on correct trials alone, however, to investigate whether the exclusion of errors

Figure 1.

Schematic of the WST and modified version used in the current study. **a.** In the classic WST participants are shown four cards (in this example, "3," "8," green and orange) and are provided with a conditional rule such as If a card shows an even number on one face, then its opposite face will be green. Participants are then asked which card(s) must be turned over to test the conditional rule provided. The only cards that can disconfirm the rule are the orange (reverse side even) and 8 (reverse side orange) cards. If the 3 card is orange on its opposite face it does not invalidate the rule (the rule does not say anything about odd cards). Likewise, if the reverse of the green card is an odd number the rule cannot be disconfirmed. **b.** Trial structure of the modified WST used in the functional magnetic resonance imaging (fMRI) study. Participants were presented with a rule (e.g., "If A then 7"), followed by a single "card," and were then asked to judge if the presented card could disconfirm the rule. By presenting cards serially the level of relational complexity needed to disconfirm the rule is manipulated on a trial-by-trial basis. [Color figure can be viewed in the online issue, which is available at wileyonlinelibrary.com.]

TABLE I. Experimental conditions in the modified WST, and examples of rules and cards

Condition	Example rule	Example card	Correct answer	Logic
Binary	If A then 7	A	This card can disconfirm the rule	The "A" card matches the first element of the rule and the reverse side (e.g., 5) can be used to disconfirm the rule. This is a binary relation.
Inverse Binary		7	Not possible to disconfirm the rule	The "7" card matches the second element of the rule and the reverse side cannot disconfirm the rule. This is a binary relation in the reverse direction defined by the rule.
Ternary		C (not-A)	Not possible to disconfirm the rule	This card contains neither of the two rule elements ("A" or "7"). The "C" card must contain a number on the reverse side, and therefore, is not informative about the rule "If A then 7." This is a ternary relation.
Quaternary		5 (not-7)	This card can disconfirm the rule	This card contains neither of the two rule elements ("A" or "7"). The "5" card must contain a letter on the reverse side. This letter could potentially be "A," therefore, disconfirming the rule "If A then 7." This is a quaternary relation.
Active control		#	—	No reasoning required.
Null	No rule presented	—	—	No reasoning required.

Note. It is important to remember that the rule is not bidirectional. In the above table "A" implies "7," but "7" does not imply "A". Therefore, showing a "7" on the reverse side of "C" is not informative, but showing "5" on the reverse of "A" is.

had any effect on changes in connectivity. First-level contrasts were used for second-level random effects analyses isolating regions showing changes in neural activity as a function of relational complexity. Specifically, we isolated the positive average card effect using a *t*-contrast (1 1 1 1 1 −5, with −5 being the null trials). The opposite contrast (−1 −1 −1 −1 −1 5) was used to isolate regions showing a negative task effect (i.e., deactivation). A *P*-value lower than 0.05, family-wise error corrected (FWE) at cluster level, was used as the threshold to declare significance. Beta regressor values were extracted from a 5 mm radius sphere located on the local maxima of each region showing a significant average effect of card complexity to explore changes in the pattern of activity as a function of complexity.

Functional interactions supporting card processing were investigated with a multiregional psychophysiological interaction (PPI) modeling approach [Cocchi et al., 2014; Gerchen et al., 2014; McLaren et al., 2012]. Instead of assessing connectivity (i.e., functional integration) between a single-seed region and all brain voxels, connectivity was assessed between pairs of regions isolated using the GLM (positive and negative average card effects). Twenty-four regions were included; 18 showed an average positive card effect (the same regions used in [Cocchi et al., 2014]) and 6 showed an average negative card effect ($P < 0.05$ FWE corrected at the cluster level, see Table II). For each participant, brain activity (first eigenvariate) was extracted from a 5 mm spherical seed region located around the peak activation voxel. As in a standard PPI analysis, the PPI signal was estimated for each region by multiplying the region's activity with the card versus the baseline regressor. Thus, the estimated PPI signal is equal to the region's activity during the processing of a specific card, but zero for all other card conditions and −1 for the baseline. Next, a GLM was used to model card-dependent influences of any given region on another. Activity within the target regions was the dependent variable. The explanatory variable was the PPI term corresponding to the source region. The card versus baseline regressor and the main effects of the psychological and physiological factors related to the activity of the region used to determine the PPI term were included as nuisance covariates. This procedure was repeated for every possible pair of regions ($24 \times 23 = 552$) in each individual card type versus rest. The result was a 24×24 connectivity matrix for each individual and card type, where each element (x,y) of the matrix stored the parameter estimate (β) for the equivalent PPI term. Unlike a regular functional connectivity analysis, this resulted in an asymmetric matrix: half the matrix contained connectivity estimates in one direction (e.g., A to B) while the second half contained connectivity estimates for the opposite direction (e.g., B to A). The β estimates quantified the card-dependent influence region x exerts

TABLE II. General linear model results used to investigate changes in task-evoked (PPI) connectivity

	Anatomy[a]			Stats[b]			
	x	y	z	K_E	Z	P_{corr}	Resting-state network[c]
Task positive ROIs (average task effect minus null trials)							
Parietal cortex	−45	−34	46	1,2636	6.84	< 0.001	Frontoparietal
	42	−55	46		5.25		
Anterior insula	−30	17	7		5.79		Cingulo-opercular
	36	14	7		5.87		
Cingulate cortex	3	8	52		5.58		
Striatum	21	5	16		6.19		
Thalamus	−15	−19	10		5.68		
Cuneus	−9	−73	10		5.51		Visual
	12	−70	13		4.95		
Lateral frontal cortex	−57	8	22		6.46		Frontoparietal
Lateral prefrontal cortex	−36	47	28		5.88		
	36	47	34		5.87		
Dorsolateral prefrontal cortex	−39	23	31		4.32		
	42	26	31		4.82		
Motor cortex	−30	−16	58		5.96		Sensorimotor
Cerebellum	3	−52	−14		6.16		
Rostrolateral prefrontal cortex	36	50	1		4.22		Frontoparietal
	−28	50	−8	62	4.41	0.07 (<0.05 FDR)	
Task Negative ROIs (null trials minus average task effect)							
Medial frontal cortex	−3	47	−8	1,916	6.10	< 0.001	Default-mode
Angular gyrus	−39	−78	30	277	6.36	< 0.001	
	48	−66	22	127	5.82	0.005	
Posterior cingulate cortex	0	−46	43	1,138	5.13	< 0.001	
Right temporal lobe	54	2	−20	145	5.10	0.002	
Left superior temporal gyrus	54	−9	−12	154	4.51	0.002	

[a]Coordinates (x, y, z) are given in Montreal Neurological Institute (MNI) atlas space.
[b]If not otherwise indicated, P values are Family-wise error (FWE) corrected for multiple comparisons at the cluster level. FDR = False Discovery Rate.
[c]ROI resting-state network allegiances are based on Dosenbach et al., [2010] (Supporting Information Table S6).

on region y. Finally, the extent of the differences in the card-evoked influence of one region on another across the five active card conditions (A, 7, C, 5, # in the example depicted in Table I) was tested using a within-subjects analysis of variance. Pairs of regions with a t-statistic exceeding an uncorrected threshold of three (equivalent to $P < 0.01$ uncorrected) were searched for complexity-modulated networks. Using the network-based statistic (NBS) a family-wise error corrected P-value ($P < 0.05$) was then attributed to each surviving network using permutation testing (10,000 permutations [Zalesky et al., 2010, 2012]). This procedure was repeated three times: once as described above, a second time using only correct trials, and a third using a different set of regions encompassing the default mode brain network (DMN) [32 regions defined by Dosenbach et al., 2010]. For this last post-hoc analysis an exploratory t-threshold of 3.5 was adopted. Brain images presented were visualized using the software Mango [Kochunov et al., 2002] and BrainNet viewer [Xia et al., 2013].

RESULTS

As reported in Cocchi et al. [2014], the mean response accuracy was above 80% in all card conditions, but declined significantly as a function of card complexity ($X^2 = 25.85$, $df = 4$, $P < 0.01$). As expected, reaction time increased significantly with card complexity ($X^2 = 21.96$, $df = 4$, $P < 0.01$).

Complexity-Induced Change in Neural Activity

In line with our original analysis [Cocchi et al., 2014], increments in card complexity increased activity within regions encompassing the frontoparietal and cingulo-opercular networks (Fig. 2a, Table II). The analyses of complexity-induced deactivations (null minus average card effect) identified a set of brain regions that are part of the default-mode brain network [Dosenbach et al., 2010; Greicius et al., 2003; Harrison et al., 2008; Power et al., 2010; Raichle et al., 2001] (Fig. 2a, details in Table II). Post hoc analysis of the condition-specific

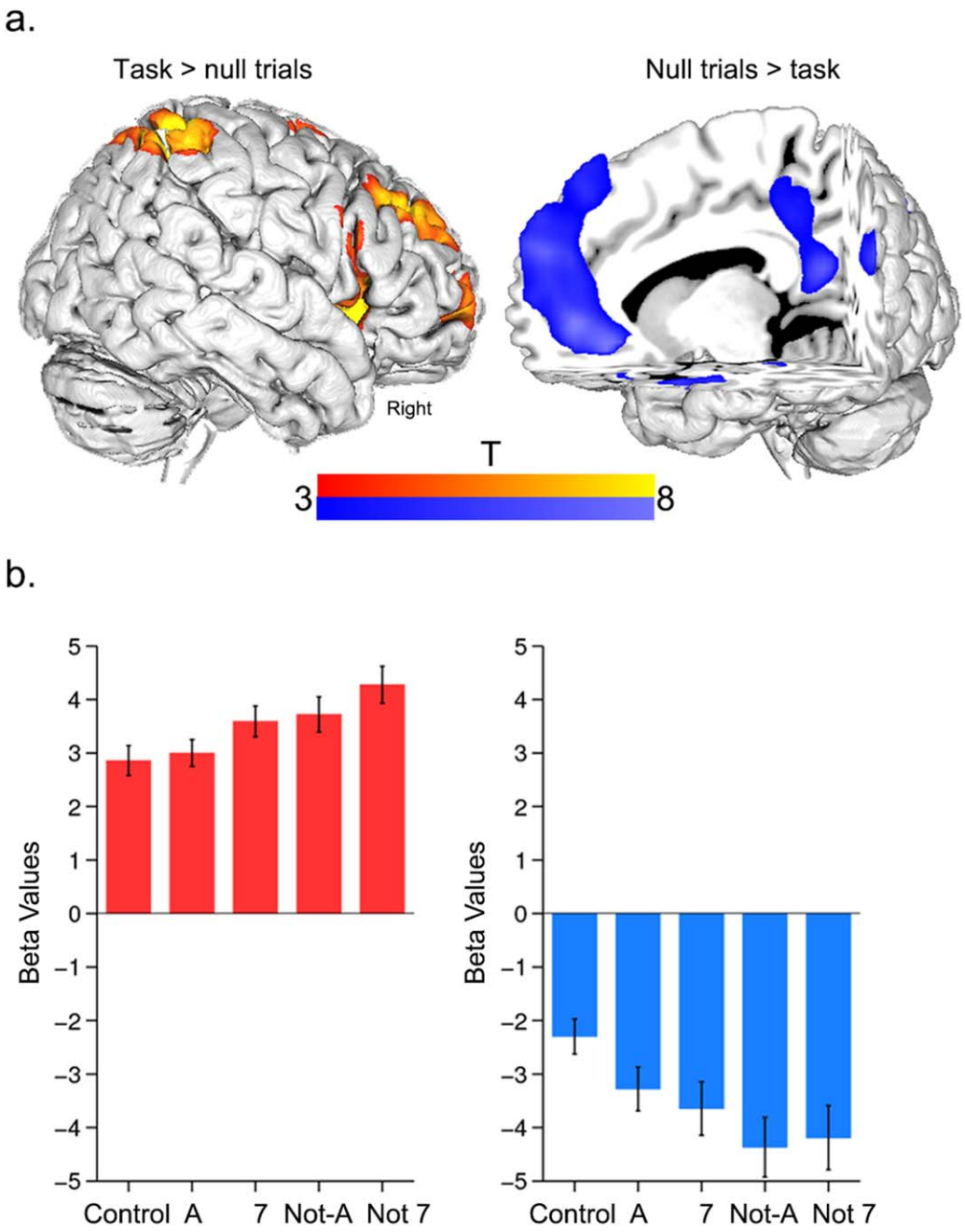

Figure 2.

Complexity-based changes in regional activity. **a.** Average brain activity during card processing. The task-positive contrast (average positive card minus null trials) showed significant neural activity in regions encompassing both frontoparietal and cingulo-opercular networks [Dosenbach et al., 2010] (see Table II for details). The task-negative contrast (null trials minus average positive card effect) showed brain regions that form part of the default-mode network [Fox et al., 2005] (Table II**)**. **b.** Mean brain activity change with increases in card complexity in task-positive and task-negative contrasts. Error bars represent the standard error of the mean. Overall, task-positive regions increased their activity as a function of card complexity. By contrast, task-negative regions decreased their activity as a function of complexity. Note that these averaged results for the group were representative for all individual regions. [Color figure can be viewed in the online issue, which is available at wileyonlinelibrary.com.]

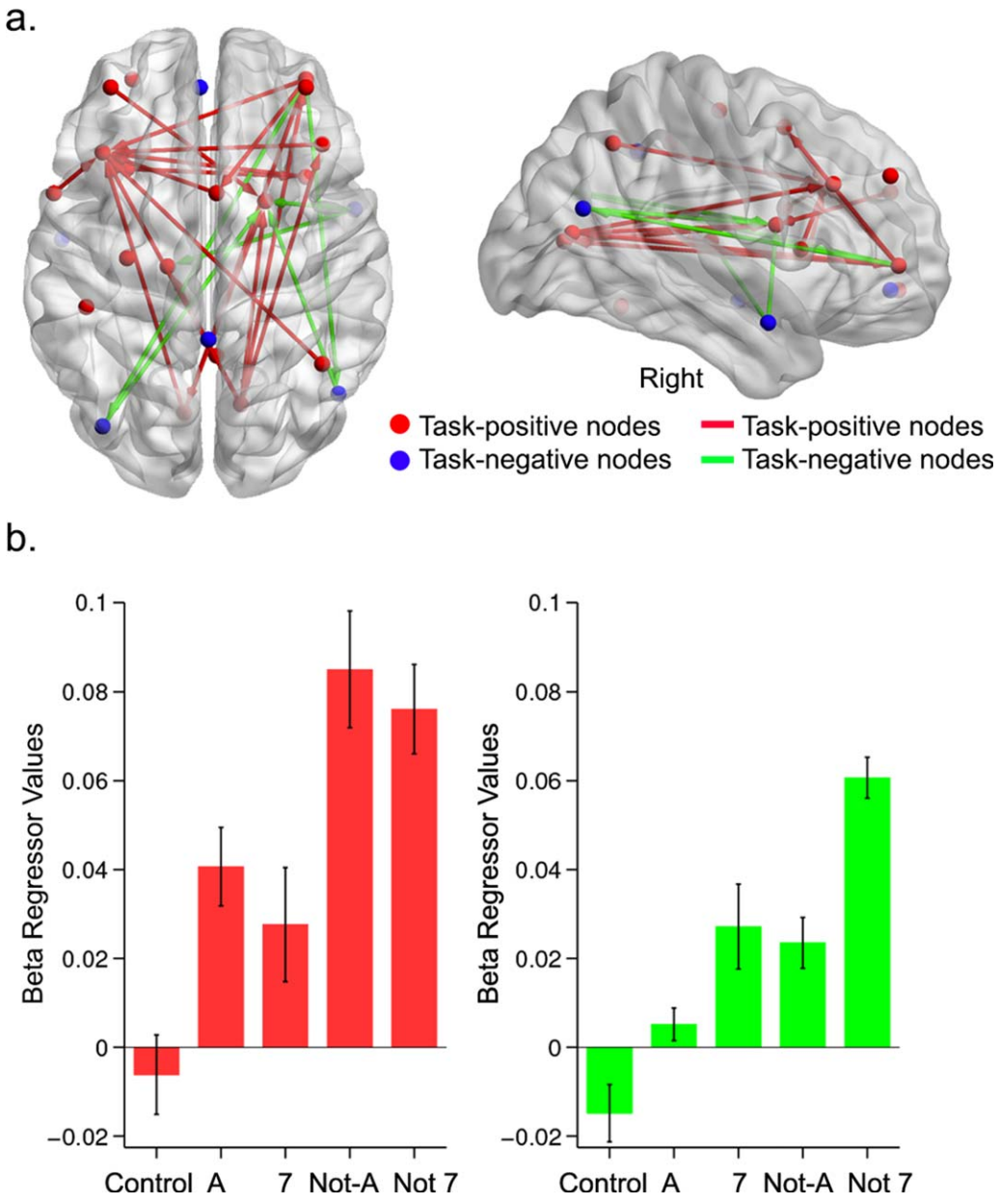

Figure 3.

Complexity-evoked changes in PPI connectivity. **a.** Red nodes correspond to task-positive regions isolated in the general linear model analysis (Figure 2; see Table II for details). Blue nodes correspond to task-negative ("deactivated") regions. The red edges indicate increases in PPI connectivity between task-positive regions, whereas the green edges represent increases in connectivity between task-positive and task-negative regions (details in Table III). **b.** Changes in average PPI connectivity values between task-positive and task-negative regions as a function of increased card complexity. Average changes were representative of edge-specific connectivity changes due to changes in complexity. [Color figure can be viewed in the online issue, which is available at wileyonlinelibrary.com.]

(e.g., "A" card vs. null card period) regional beta regressor values showed a significant parametric decrease in activity as a function of increasing relational complexity (Fig. 2b).

Complexity-Induced Change in PPI Connectivity

PPI connectivity analysis revealed a significant increase in integration between cingulo-opercular, frontoparietal,

TABLE III. Pairwise change in PPI functional connectivity between source and target regions as a function of relational complexity

Source region	Target region	Direction of change
Task positive—task positive connections		
Left anterior insula	Right anterior insula	Increasing
	Left dorsolateral prefrontal cortex	
Right anterior insula	Left dorsolateral prefrontal cortex	
Cingulate cortex	Left dorsolateral prefrontal cortex	
Left cuneus	Striatum	
	Left dorsolateral prefrontal cortex	
Right cuneus	Striatum	
	Thalamus	
	Left dorsolateral prefrontal cortex	
	Right dorsolateral prefrontal cortex	
	Left rostrolateral prefrontal cortex	
Right dorsolateral prefrontal cortex	Left dorsolateral prefrontal cortex	
Lateral frontal cortex	Left dorsolateral prefrontal cortex	
Left lateral prefrontal cortex	Striatum	
Right parietal cortex	Left dorsolateral prefrontal cortex	
Right rostrolateral prefrontal cortex	Cingulate cortex	
	Left cuneus	
	Right cuneus	
	Left dorsolateral prefrontal cortex	
Task negative—task positive connections		
Angular gyrus left	Striatum	Increasing
Angular gyrus right	Striatum	
Temporal pole right	Striatum	
	Thalamus	
Right rostrolateral prefrontal cortex	Angular gyrus left	
	Angular gyrus right	

Note. Connections were corrected at the network level using NBS ($P < 0.05$ FWE) [Zalesky et al., 2010, 2012].

and default-mode regions as a function of increased card complexity (Fig. 3a and Table III). Although the PPI analysis was performed on a larger set of regions, changes in connectivity between frontoparietal and cingulo-opercular regions replicated our previously reported results [Cocchi et al., 2014] (red edges in Fig. 3a, Table III). There was also a significant modulation in complexity-evoked connectivity between discrete regions encompassing task-positive and default-mode networks (green edges in Fig. 3b, Table III). Specifically, integration between the angular gyri and the striatum progressively increased as a function of relational complexity. The two angular gyri also showed increased integration with the rostrolateral prefrontal cortex. A similar pattern of results was found between the right temporal pole (one of the task-negative regions, see Table II) and the thalamus and striatum. It is important to note that NBS only allows inferences at the level of the whole network ($P < 0.05$ FWE). As such, while the detected edge-specific effects were consistent and relatively robust (partial Eta-squared > 0.13, $P < 0.02$ uncorrected), inferences on the functional significance of such specific complexity-evoked connectivity changes need to be drawn with caution.

Within the network of interest, there was no change in integration as a function of complexity between regions showing significant deactivations with complexity (blue spheres in Fig. 3a). A follow-up analysis was performed to further investigate the nature of this unexpected result (see below).

When only correct trials were included in the PPI analysis, a similar network and pattern of connectivity changes were observed. The only exception was the absence of a complexity-based increase in PPI connectivity between the left rostrolateral prefrontal cortex and the angular gyri (Figure 3a).

Follow-Up Analysis of Default-Mode Network Dynamics as a Function of Complexity

We found no change in connectivity within the default-mode network as a function of increasing task complexity. This result was unexpected, but might be due to our approach of selecting the regions of interest based on complexity-evoked activation [Gerchen et al., 2014]. Likewise, the default-mode network is thought to be comprised of functionally heterogeneous subnetworks [Andrews-

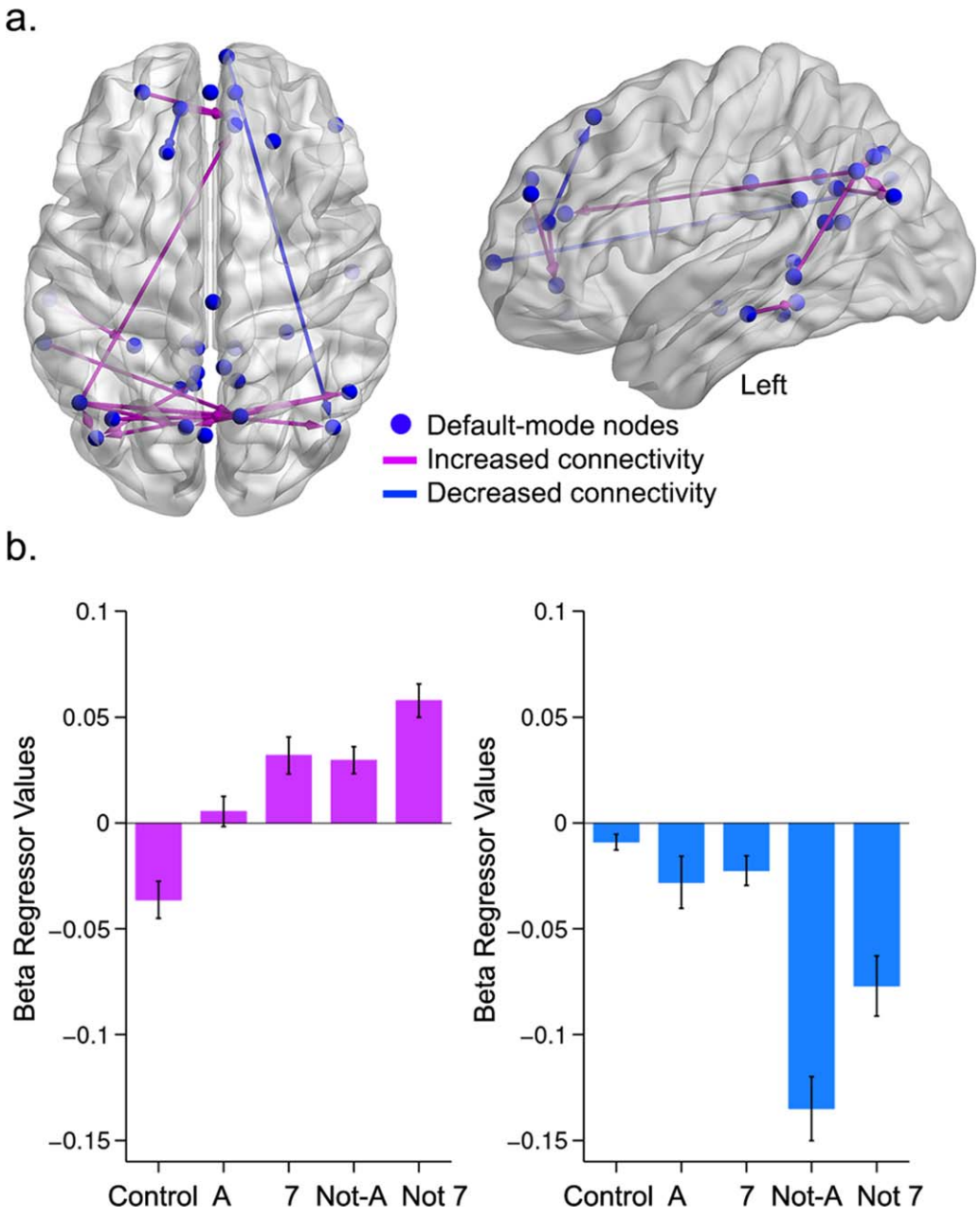

Figure 4.

Complexity-evoked changes in PPI connectivity within the default-mode network. ***a.*** Purple edges indicate increased PPI connectivity as a function of complexity, whereas blue edges represent decreased connectivity (details in Table IV). **b**. Average PPI connectivity patterns for pairwise connections showing an increase in connectivity (in purple) and decreased connectivity (in blue) as a function of increased relational complexity. [Color figure can be viewed in the online issue, which is available at wileyonlinelibrary.com.]

Hanna et al., 2010; Eldaief et al., 2011]. The fact that regions were selected based on complexity-induced neural activations may, therefore, have biased our selection toward one or more specific subnetwork(s). As such, it is possible that complexity-induced deactivations did not capture complexity-induced network dynamics in full. To test this hypothesis, we performed the same PPI connectivity analysis using 32 regions of interest encompassing the current

TABLE IV. Pairwise change in PPI functional connectivity between source and target regions encompassing the default-mode network as a function of relational complexity

Source region	Target region	Direction of change
Default-mode regions		
Anterior prefrontal cortex	Ventral medial prefrontal cortex	Increasing
Ventral medial prefrontal cortex		
Left angular gyrus	Anterior cingulate cortex	
Left inferior temporal	Left occipital cortex	
Left occipital cortex	Right Angular gyrus	
Left occipital cortex	Left Angular gyrus	
Left inferior temporal cortex	Precuneus	
Left angular gyrus		
Intra parietal sulcus		
Right angular gyrus	Medial occipital cortex	
Left a ngular gyrus		
Left angular gyrus	Right occipital cortex	
Precuneus	Left occipital cortex	
Right angular gyrus		
Left angular gyrus		
Ventral medial prefrontal cortex	Right occipital cortex	Decreasing
Ventral medial prefrontal cortex	Superior frontal cortex	

Note. Connections were corrected at the network level using NBS ($P < 0.05$ FWE) [Zalesky et al., 2010, 2012].

task-negative network and the wider default mode network as defined by Dosenbach et al. [2010] (see Supporting Information Table S1 for details of the locations of the regions).

Result showed that increased task complexity induced two distinct sets of changes within default-mode network dynamics (Fig. 4, Table IV). A first set of regions, primarily consisting of the bilateral angular gyri, precuneus, occipital cortex, and medial prefrontal cortex, showed an increase in functional connectivity as a function of card complexity (purple connections in Fig. 4). Conversely, a small subset of regions showed a decrease in integration as card complexity increased (blue connections in Fig. 4). Our findings also suggest that the angular gyri were involved in both types of dynamics, as well as in cross-network integration (i.e., DMN-control networks, Fig. 3). Note that there was also a small set of connections within the network that did not show a consistent increase or decrease in PPI connectivity across increasing reasoning complexity (see Supporting Information Fig. S1).

DISCUSSION

The aim of this study was to assess changes in the functional interplay between brain areas showing increased or decreased neural activity as a function of increasing complexity in a well-known cognitive reasoning task. Specifically, we tested whether performance is underpinned by a consistent anticorrelation between regions within the default-mode and control networks, or, alternatively, whether emergent integration between these networks arises in response to increasing relational complexity.

Task-induced reductions ("deactivations") in neural activity as a function of cognitive load have been consistently observed in brain areas within the default-mode network [Lawrence et al., 2003; McKiernan et al., 2003; Sonuga-Barke and Castellanos, 2007]. Such context-driven deactivations are thought to accompany shifts in attentional focus between self-directed mental activity and external stimuli and tasks. Consistent with this notion, it has been shown that deactivation within default-mode regions becomes more pronounced when interoceptive thoughts are reduced and task difficulty increases [Lawrence et al., 2003; McKiernan et al., 2003, 2006]. Likewise, individuals with attentional problems show reduced segregation (anticorrelation) between regions of the control and default-mode networks [Chabernaud et al., 2012; Cocchi et al., 2012]. Together, these observations have led to the view that segregation or antagonism between default-mode and task-positive regions is a predictor of optimal cognitive performance [Anticevic et al., 2012; Fox et al., 2005; Sonuga-Barke and Castellanos, 2007]. Recent findings have challenged this view, however, suggesting instead that in some task contexts performance may be supported by transient cooperation—or reduced antagonism—between regions that are otherwise segregated in a state of rest [Fornito et al., 2012; Leech et al., 2011, 2012; Liang et al., in press]. The current study further adds to this literature by showing that increasing cognitive demands in a reasoning task is accompanied by a loss of segregation and a progressive enhancement of connectivity between regions within control and default-mode networks. These changes co-occurred alongside an increased functional

interplay between frontoparietal and cingulo-opercular regions [Cocchi et al., 2014].

The current results show that parametric increases in task complexity proportionally enhance integration between regions demonstrating either a local increase (striatum and thalamus) or decrease (angular gyri and right temporal pole) in neural activity. The pattern of network-level connectivity revealed here is consistent with previous results suggesting that the striatum and the thalamus are functionally and anatomically related to cortical structures supporting cognitive control functions [Haber, 2003; Haber and Knutson, 2010]. Increased striatal activity is critical to the performance of cognitive control tasks [Bunge and Wright, 2007; Mestres-Misse et al., 2012]. Likewise, striatal activity appears important for rapidly linking acquired representations with specific actions [Bunge et al., 2005; Pasupathy and Miller, 2005]. Our findings go beyond these observations by suggesting that the striatum and the thalamus are key relays for facilitating enhancement of task-related processes, as well as suppression of task-unrelated processes. This hypothesis is consistent with recent evidence that the caudate and thalamus are transitional nodes that change their coupling with control and default-mode networks as a function of task demands [Dwyer et al., 2014]. Although the PPI method does not allow an unequivocal assessment of causal interactions between distinct neural populations, our results suggest that deactivation of specific default-mode regions may drive the initiation of frontoparietal and cingulo-opercular activity via the basal ganglia (Table III). Likewise, increased functional integration between default-mode areas and the basal ganglia may be essential to manage the integration of self-referential processes during task performance.

Greater task complexity was also related to increased connectivity between the right rostrolateral prefrontal cortex and the angular gyrus, bilaterally. The rostrolateral prefrontal cortex is involved in delayed, context-specific implementation of acquired rules [Gilbert, 2011; Koechlin et al., 1999; Sakai and Passingham, 2003]. We have suggested that, alongside neurons within the anterior insular cortex [Menon and Uddin, 2010], neurons within this anterior prefrontal region play an important role in managing the task-based interplay between frontoparietal and cingulo-opercular networks [Cocchi et al., 2014]. While inferences on pairwise changes in connectivity need to be interpreted cautiously, the current findings suggest that the right rostrolateral prefrontal cortex might be involved in managing the engagement and disengagement of diffuse patterns of activity within the default-mode network. When only correct trials were included in our analyses, connectivity changes between the rostrolateral prefrontal cortex and the angular gyri were absent. Other than this discrete change in connectivity, the topology of the resulting network was identical to the network isolated when including both correct and error trials. This result is unlikely to be due to the small reduction in statistical power, as participants maintained mean accuracy above 80% in all card conditions. Rather, it suggests that increased integration between the rostrolateral prefrontal cortex and default-mode regions as a function of increased task complexity may be related to contamination of task-unrelated activity with task-relevant processes [Christoff et al., 2009; Weissman et al., 2006]. As such, default-mode interference with rostrolateral prefrontal cortex activity may cause, or be the consequence of, increased difficulties in efficiently managing the cingulo-opercular (task-set) and frontoparietal (trial-by-trial control) dynamics. These results encourage further investigation of the task-based interplay between default-mode and rostrolateral prefrontal cortex as a function of cognitive load.

Previous studies have suggested that cognitive task performance is accompanied by an increase in integration between default-mode regions [Hampson et al., 2006]. The generalizability of these findings has been challenged by evidence suggesting that the default-mode network may be comprised of subnetworks that have distinct functional roles in different task contexts [Andrews-Hanna et al., 2010]. Our analyses support the latter hypothesis by showing that functional integration within regions of the default mode network may either increase or decrease as a function of task complexity. Our findings also highlight a role for the angular gyrus in managing complexity-based integration and segregation within the default-mode network, and between the default-mode and control networks.

In summary, the current study highlights the dynamic functional interplay between default-mode and control networks as a function of increased reasoning complexity. Our findings challenge the notion that functional segregation between these networks invariably supports cognitive task performance. By contrast, the results provide further evidence in favor of recent accounts which suggest that transient cooperation between regions encompassing default-mode and control networks is critical to performing challenging cognitive tasks [Cocchi et al., 2013]. We have also shown that the striatum and thalamus play an important part in managing interactions between control and default-mode processes during cognitive reasoning.

REFERENCES

Andrews-Hanna JR, Reidler JS, Sepulcre J, Poulin R, Buckner RL (2010): Functional-anatomic fractionation of the brain's default network. Neuron 65:550–562.

Anticevic A, Cole MW, Murray JD, Corlett PR, Wang XJ, Krystal JH (2012): The role of default network deactivation in cognition and disease. Trends Cogn Sci 16:584–592.

Bluhm RL, Clark CR, McFarlane AC, Moores KA, Shaw ME, Lanius RA (2011): Default network connectivity during a working memory task. Hum Brain Mapp 32:1029–1035.

Bunge SA, Wright SB (2007): Neurodevelopmental changes in working memory and cognitive control. Curr Opin Neurobiol 17:243–250.

Bunge SA, Wallis JD, Parker A, Brass M, Crone EA, Hoshi E, Sakai K (2005): Neural circuitry underlying rule use in humans and nonhuman primates. J Neurosci 25:10347–10350.

Chabernaud C, Mennes M, Kelly C, Nooner K, Di Martino A, Castellanos FX, Milham MP (2012): Dimensional brain-behavior relationships in children with attention-deficit/hyperactivity disorder. Biol Psychiatry 71:434–442.

Christoff K, Gordon AM, Smallwood J, Smith R, Schooler JW (2009): Experience sampling during fMRI reveals default network and executive system contributions to mind wandering. Proc Natl Acad Sci USA 106:8719–8724.

Cocchi L, Bramati IE, Zalesky A, Furukawa E, Fontenelle LF, Moll J, Tripp G, Mattos P (2012): Altered functional brain connectivity in a non-clinical sample of young adults with attention-deficit/hyperactivity disorder. J Neurosci 32:17753–17761.

Cocchi L, Zalesky A, Fornito A, Mattingley JB (2013): Dynamic cooperation and competition between brain systems during cognitive control. Trends Cogn Sci 17:493–501.

Cocchi L, Halford GS, Zalesky A, Harding IH, Ramm BJ, Cutmore T, Shum DH, Mattingley JB (2014): Complexity in relational processing predicts changes in functional brain network dynamics. Cereb Cortex 24:2283–2296.

Cole MW, Reynolds JR, Power JD, Repovs G, Anticevic A, Braver TS (2013): Multi-task connectivity reveals flexible hubs for adaptive task control. Nat Neurosci 16:1348–1355.

Cole MW, Bassett DS, Power JD, Braver TS, Petersen SE (2014): Intrinsic and task-evoked network architectures of the human brain. Neuron 83:238–251.

Dosenbach NU, Visscher KM, Palmer ED, Miezin FM, Wenger KK, Kang HC, Burgund ED, Grimes AL, Schlaggar BL, Petersen SE. (2006): A core system for the implementation of task sets. Neuron 50:799–812.

Dosenbach NU, Nardos B, Cohen AL, Fair DA, Power JD, Church JA, Nelson SM, Wig GS, Vogel AC, Lessov-Schlaggar CN, Barnes KA, Dubis JW, Feczko E, Coalson RS, Pruett JR Jr, Barch DM, Petersen SE, Schlaggar BL. (2010): Prediction of individual brain maturity using fMRI. Science 329:1358–1361. Erratum in: Science. 2010 Nov 5;330(6005):756.

Dosenbach NU, Nardos B, Cohen AL, Fair DA, Power JD, Church JA, Nelson SM, Wig GS, Vogel AC, Lessov-Schlaggar CN and others (2010): Prediction of individual brain maturity using fMRI. Science 329:1358–1361.

Dwyer DB, Harrison BJ, Yücel M, Whittle S, Zalesky A, Pantelis C, Allen NB, Fornito A (2014): Large-scale brain network dynamics supporting adolescent cognitive control. J Neurosci 34:14096–14107.

Eldaief MC, Halko MA, Buckner RL, Pascual-Leone A (2011): Transcranial magnetic stimulation modulates the brain's intrinsic activity in a frequency-dependent manner. Proc Natl Acad Sci USA 108:21229–21234.

Fornito A, Harrison BJ, Zalesky A, Simons JS (2012): Competitive and cooperative dynamics of large-scale brain functional networks supporting recollection. Proc Natl Acad Sci USA 109: 12788–12793.

Fox MD, Snyder AZ, Vincent JL, Corbetta M, Van Essen DC, Raichle ME (2005): The human brain is intrinsically organized into dynamic, anticorrelated functional networks. Proc Natl Acad Sci USA 102:9673–9678.

Gerchen MF, Bernal-Casas D, Kirsch P (2014): Analyzing task-dependent brain network changes by whole-brain psychophysiological interactions: A comparison to conventional analysis. Hum Brain Mapp 35:5071–5082.

Gilbert SJ (2011): Decoding the content of delayed intentions. J Neurosci 31:2888–2894.

Greicius MD, Krasnow B, Reiss AL, Menon V (2003): Functional connectivity in the resting brain: A network analysis of the default mode hypothesis. Proc Natl Acad Sci USA 100:253–258.

Haber SN (2003): The primate basal ganglia: Parallel and integrative networks. J Chem Neuroanat 26:317–330.

Haber SN, Knutson B (2010): The reward circuit: Linking primate anatomy and human imaging. Neuropsychopharmacology 35: 4–26.

Halford GS, Wilson WH, Phillips S (1998): Processing capacity defined by relational complexity: Implications for comparative, developmental, and cognitive psychology. Behav Brain Sci 21: 803–831; discussion 831–864.

Halford GS, Wilson WH, Phillips S (2010): Relational knowledge: The foundation of higher cognition. Trends Cogn Sci 14:497–505.

Hampson M, Driesen NR, Skudlarski P, Gore JC, Constable RT (2006): Brain connectivity related to working memory performance. J Neurosci 26:13338–13343.

Harrison BJ, Pujol J, Lopez-Sola M, Hernandez-Ribas R, Deus J, Ortiz H, Soriano-Mas C, Yucel M, Pantelis C, Cardoner N (2008): Consistency and functional specialization in the default mode brain network. Proc Natl Acad Sci USA 105:9781–9786.

Johnson-Laird PN (2010): Mental models and human reasoning. Proc Natl Acad Sci USA 107:18243–18250.

Kelly AM, Uddin LQ, Biswal BB, Castellanos FX, Milham MP (2008): Competition between functional brain networks mediates behavioral variability. Neuroimage 39:527–537.

Koechlin E, Basso G, Pietrini P, Panzer S, Grafman J (1999): The role of the anterior prefrontal cortex in human cognition. Nature 399:148–151.

Kochunov P, Lancaster J, Thompson P, Toga AW, Brewer P, Hardies J, Fox P. (2002): An optimized individual target brain in the Talairach coordinate system. NeuroImage 17:922–927.

Lawrence NS, Ross TJ, Hoffmann R, Garavan H, Stein EA (2003): Multiple neuronal networks mediate sustained attention. J Cogn Neurosci 15:1028–1038.

Leech R, Kamourieh S, Beckmann CF, Sharp DJ (2011): Fractionating the default mode network: Distinct contributions of the ventral and dorsal posterior cingulate cortex to cognitive control. J Neurosci 31:3217–3224.

Leech R, Braga R, Sharp DJ (2012): Echoes of the brain within the posterior cingulate cortex. J Neurosci 32:215–222.

Liang X, Zou Q, He Y, Yang Y: Topologically reorganized connectivity architecture of default-mode, executive-control, and salience networks across working memory task loads (in press).

McKiernan KA, Kaufman JN, Kucera-Thompson J, Binder JR (2003): A parametric manipulation of factors affecting task-induced deactivation in functional neuroimaging. J Cogn Neurosci 15:394–408.

McKiernan KA, D'Angelo BR, Kaufman JN, Binder JR (2006): Interrupting the "stream of consciousness": An fMRI investigation. Neuroimage 29:1185–1191.

McLaren DG, Ries ML, Xu G, Johnson SC (2012): A generalized form of context-dependent psychophysiological interactions (gPPI): A comparison to standard approaches. Neuroimage 61:1277–1286.

Menon V, Uddin LQ (2010): Saliency, switching, attention and control: A network model of insula function. Brain Struct Funct 214:655–667.

Mestres-Misse A, Turner R, Friederici AD (2012): An anterior-posterior gradient of cognitive control within the dorsomedial striatum. Neuroimage 62:41–47.

Pasupathy A, Miller EK (2005): Different time courses of learning-related activity in the prefrontal cortex and striatum. Nature 433:873–876.

Popa D, Popescu AT, Pare D (2009): Contrasting activity profile of two distributed cortical networks as a function of attentional demands. J Neurosci 29:1191–1201.

Power JD, Fair DA, Schlaggar BL, Petersen SE (2010): The development of human functional brain networks. Neuron 67:735–748.

Raichle ME, MacLeod AM, Snyder AZ, Powers WJ, Gusnard DA, Shulman GL (2001): A default mode of brain function. Proc Natl Acad Sci USA 98:676–682.

Sakai K, Passingham RE (2003): Prefrontal interactions reflect future task operations. Nat Neurosci 6:75–81.

Sonuga-Barke EJ, Castellanos FX (2007): Spontaneous attentional fluctuations in impaired states and pathological conditions: A neurobiological hypothesis. Neurosci Biobehav Rev 31:977–986.

Sridharan D, Levitin DJ, Menon V (2008): A critical role for the right fronto-insular cortex in switching between central-executive and default-mode networks. Proc Natl Acad Sci USA 105:12569–12574.

Wason P (1968): Reasoning about a rule. Q J Exp Psychol 20:273–281.

Wason PC (1966): Reasoning. In: Foss BM, editor. New Horizons in Psychology. Harmondsworth: Penguin.

Weissman DH, Roberts KC, Visscher KM, Woldorff MG (2006): The neural bases of momentary lapses in attention. Nat Neurosci 9:971–978.

Xia M, Wang J, He Y (2013): BrainNet Viewer: A network visualization tool for human brain connectomics. PLoS One 8:e68910.

Zalesky A, Fornito A, Bullmore ET (2010): Network-based statistic: Identifying differences in brain networks. Neuroimage 53: 1197–1207.

Zalesky A, Cocchi L, Fornito A, Murray MM, Bullmore E (2012): Connectivity differences in brain networks. Neuroimage 60: 1055–1062.